Charge-charge coupling effects on dipole emitter relaxation within a classical electron-ion plasma description

Emmanuelle Dufour, Annette Calisti, and Bernard Talin
UMR6633, Université de Provence, Centre Saint Jérôme, 13397 Marseille Cedex 20, France

Marco A. Gigosos and Manuel A. González
Departamento de Óptica y Física Aplicada, Facultad de Ciencias, Universidad de Valladolid, 47071 Valladolid, Spain

Teresa del Río Gaztelurrutia
Escuela Superior de Ingenieros, Ald. Urquijo s/n 48013 Bilbao, Spain

James W. Dufty
Department of Physics, University of Florida, Gainesville, Florida 32611, USA
(Received 11 August 2004; revised manuscript received 25 March 2005; published 24 June 2005)

Studies of charge-charge (ion-ion, ion-electron, and electron-electron) coupling properties for ion impurities in an electron gas are carried out on the basis of a regularized electron-ion potential without short-range Coulomb divergence. This work is motivated, in part, by questions arising from recent spectroscopic measurements revealing discrepancies with present-day theoretical descriptions. Many of the current radiative property models for plasmas include only single electron-emitter collisions and neglect some or all charge-charge interactions. A molecular-dynamics simulation of dipole relaxation is proposed here to allow proper account of many electron-emitter interactions and all charge-charge couplings. As illustrations, molecular-dynamics simulations are reported for the cases of a single ion embedded in an electron plasma and for a two-component ion-electron plasma. Charge-charge coupling effects are discussed for hydrogenlike Balmer α lines at weak coupling conditions.

DOI: 10.1103/PhysRevE.71.066409 PACS number(s): 52.65.Yy, 52.25.Vy, 05.10.−a

I. INTRODUCTION

Atoms or ion emitters in plasmas undergo perturbations inducing broadening and shift of natural emission lines. The magnitudes of these effects, dependent on plasma composition, temperature, and density, are actually used for diagnosing plasma conditions. Besides the Doppler effect, related to thermal motion, perturbations on the emitter due to surrounding ions and electrons give rise to Stark effect, resulting in line broadening and shift. Doppler effect is used to investigate the emitter temperature while Stark effect is linked to the amount of charge around the emitter, usually characterized by the free electron density.

In order to use these physical processes in a diagnostic technique, accurate models that connect spectral line shapes to plasma composition, density, and temperature are required. Most of such models, which allow to synthesize line shapes, have been developed in the last fifty years on the basis of semi-classical approaches [1–4]. Semiclassical refers in this context to models where, on the one hand, the quantum atomic structure of the emitter does not depend on the plasma, and on the other, the surrounding plasma depends only on the emitter charge but not on the internal state of the emitter. Line shapes broadened by Stark effect are predicted by modeling the line emission as the quantum system undergoes a classical electric perturbation because of the surrounding ions and electrons. Within the framework of this semiclassical approach further approximations have been considered. For example, it is quite usual to treat independently fast electrons (i.e., high-frequency perturbation) and slow ions (i.e., low-frequency perturbation). More recent numerical approaches based on computer simulation consider electron and ion perturbations at the same level.

The so-called ion-dynamics effect on line shapes has been successfully interpreted via computer simulation [5]. In this way, improved data bases for hydrogen line broadening have been built for diagnostic purposes [6]. In these calculations, simulations are based on independent particle models. The charge-charge coupling [7] is approximated using interactions with the emitter screened at Debye length. These calculations are designed mainly for arc plasma conditions—weak coupling conditions—and for charged or neutral emitters, and become questionable when increasing electron densities or lower electron temperatures are considered.

For increasing plasma coupling, there arise discrepancies between independent particle model calculations and the experiments. For example, there are still discussions on the interpretation of Balmer α experiments for neutral hydrogen [8]. The same occurs in the case of charged emitters, where, for example, the expected $1/Z^2$ behavior for linewidths within an isoelectronic series is not observed in experiments [9].

A first step to improve those techniques is the use of molecular-dynamics (MD) simulations where interactions between all particles, including emitters, are taken into account [5]. The intention of this work is to analyze the effect that correlations between charges induce on Stark broadening spectra. The work concentrates on the case of one

 ©2005 The American Physical Society

charged emitter in perturbing electrons (one-component plasma with an impurity of opposite charge) with the objective to estimate the effect equivalent to what is usually approximated via Debye screening in independent-particle simulations. Simulations in neutral two-component plasmas have also been performed. Although they are not reported with detail, one result is mentioned hereafter.

Computer simulations are used as an ideal laboratory experiment that allows one to isolate phenomena and thus separately analyze effects of coupling between perturbing electrons and between electrons and the emitting ion. Only weak coupling conditions have been considered ($0.03<\Gamma<0.13$), but charge-charge coupling phenomena are illustrated well enough.

It is well known that in molecular-dynamics calculations, where particles of opposite charge are involved, the use of regularized potentials is essential so that Coulomb divergences at short distances are avoided [10,11]. This regularization reproduces, in an approximate way, quantum diffraction in the collision between a free electron and an ion. Similar results could be obtained with other regularized Coulomb potential. Obviously, the regularization is only relevant for distances much shorter than the average distance between particles. For the sake of simplicity, the interaction between charges of the same sign is not regularized, since, due to repulsive forces, numerical divergences at short distances are improbable.

Molecular dynamics is used in a conventional way. Particles are inside a cube with periodic boundary conditions [12]. Each particle interacts with all the particles within a sphere centered on it. The radius of the sphere is chosen to be half the size of the cube. This actually corresponds to a large distance regularization of the Coulomb potential.

Stability and suitability of the simulations are controlled, monitoring total energy stationarity and the behavior of three characteristic functions: the statistical distribution of the electric field at the ion, the electric field correlation function (FCF), and the ion-electron pair correlation function $g(r)$. As an additional control, this last function can be compared to results of the hypernetted chain approximation (HNC) [13,14]. All these functions provide us with both the static and dynamic properties of the electric field, which originates spectral line broadening. This time-dependent field is saved and later on used in calculations of Stark spectra. The weak-coupling physical conditions that have been considered a guarantee that a quantum treatment of the detailed collision processes is not necessary for the present objective. Therefore, comparisons of the results of this work, such as short-distance electron density or electron-ion pseudopotential, with density-functional theories or quantum treatments of the same kind [15–17], are unnecessary.

In this paper, the effects of dynamical screening on the charge correlation are described first. In this way the use of Debye screening in independent-particle simulations is justified *a posteriori*. Then the validity of the fast-fluctuation model, where line broadening is proportional to the time integral of the perturbing field correlation, is analyzed. Finally, the influence that the emitter charge has on the field correlation and, as a consequence, on the width of spectral lines, is studied. In this later case, to simplify the treatment, the Balmer α line of hydrogenlike ions with ionic charge $Z=1$, 3, 5, and 8 is considered.

II. PLASMA ENVIRONMENT MODELING

In the density and temperature conditions considered in this paper, the repulsive interaction between charges of the same sign effectively excludes pair configurations of the order of the DeBroglie wavelength, guaranteeing that quantum effects are small. Consequently, the ion-ion, ion-emitter, and electron-electron interactions are taken to be Coulomb

$$V_{12}(r) = Z_1 Z_2 e^{-r/\lambda}/r, \tag{1}$$

where $Z_1 Z_2$ is positive. For practical purposes, these Coulomb interactions have been screened at a distance $\lambda \simeq s/2$, of the order of the cubic cell size s. This screening allows application of the usual periodic boundary conditions in MD simulation. Since interactions among charges introduce a physical screening at much shorter distances, the introduction of screening at $\lambda = s/2$ does not affect any of the properties considered in this work.

In contrast, electron-ion interactions are attractive and therefore configurations involving electrons at distances of the order of the DeBroglie wavelength or shorter have to be considered. At such distances, the Coulomb interaction must be modified in a classical description, to account for quantum diffraction effects. There are many ways such quantum potentials can be constructed, and here we use one of the simplest forms [10]

$$V_{ie}(r) = -Ze^2(1 - e^{-r/\delta})e^{-r/\lambda}/r, \tag{2}$$

where $\delta = (2\pi\hbar^2/m_e k_B T_e)^{1/2}$ is the thermal DeBroglie wavelength. This ion-electron potential regularization provides well-defined classical physics for opposite-sign charge systems, and allows the application of the various sophisticated classical N-body methods of classical statistical mechanics [11,14,18].

Other parameters of interest are the average electron-electron distance, $r_0 = (3/4\pi N_e)^{1/3}$, defined in terms of the electron density N_e; the electron thermal velocity $v_0 = (2k_B T_e/m_e)^{1/2}$; the mean electronic field $E_0 = e/r_0^2$; the electron-electron coupling constant $\Gamma = e^2/r_0 k_B T_e$; and the electron plasma frequency $\omega_p = (4\pi N_e e^2/m_e)^{1/2}$. Molecular-dynamics simulations are carried out using N electrons with a unique charged emitter, or N electrons and N/Z_i ions in the case of the two-component plasma (TCP). When a uniform positive background is required to maintain overall charge neutrality, it has no effect on particle motion since the charges move across an infinite system. As we are only interested in the charge structure and dynamics in the ion vicinity, the usual Ewald's sums are not required. Particle motion in the MD simulation is achieved using a Verlet's algorithm with a time-step error of order $(\Delta t)^4$: $\mathbf{r}_{n+1} = 2\mathbf{r}_n - \mathbf{r}_{n-1} + \mathbf{a}_n(\Delta t)^2$. Finally, the initial conditions of the simulations are set up in such a way that the total energy fluctuations remain very small during the whole evolution of the system, without the need of any external temperature control (no thermostat).

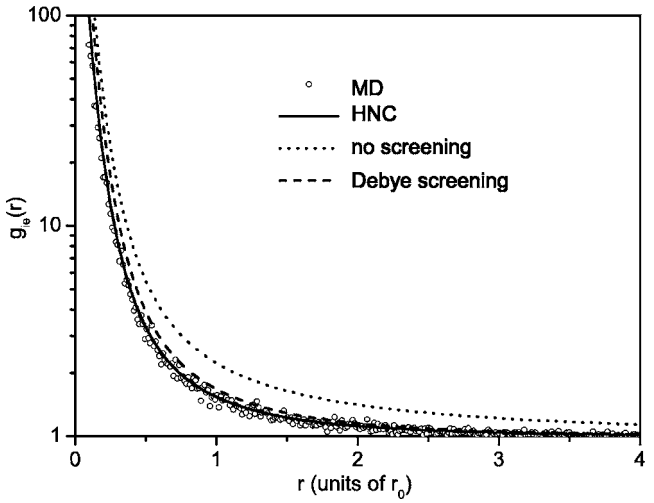

FIG. 1. Ion-electron pair correlation function at $N_e=10^{19}$ cm^{-3}, $T_e=50000$ K, $Z=8$, and $\delta\simeq 0.1r_0$. Solid line: HNC; circles: MD with all coupling; dashed: Debye screened independent electrons; dotted: noninteracting electrons moving in the ion field.

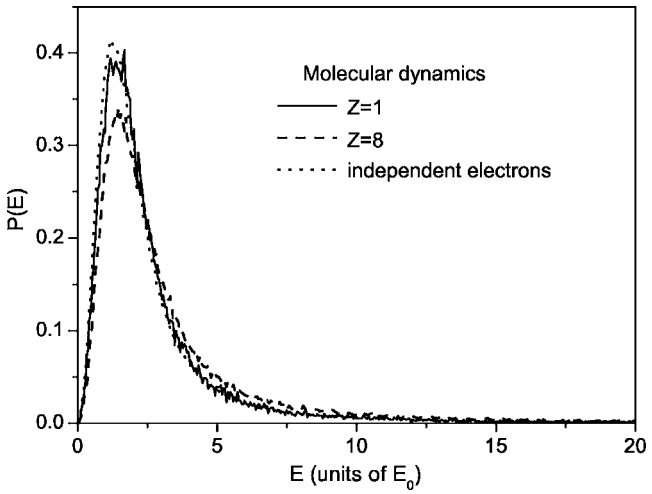

FIG. 2. Field distribution at $N_e=10^{19}$ cm^{-3}, $T_e=200\,000$ K. Solid: $Z=1$; dashed: $Z=8$; dotted: independent electrons.

A. Unique ion emitter in an electron gas

Ion-electron and electron-electron interactions affect both static and dynamic properties of the electrons near the impurity ion. Ion-electron coupling determines the dominant Z dependence of these properties, whereas electron-electron coupling controls screening and other quantitative effects. In this work, the electron density, electric microfield distribution, and electric field autocorrelation function have been studied for various values of temperature, density, and impurity charge number Z. The main statistical properties of the electron structure close to the ion (e.g., electron density, electric field probability distribution) are derived using both MD simulation and the HNC integral equations. Here, HNC is specialized for the single impurity case, i.e., for a vanishing ion density [14]. The impurity-electron correlation function $g_{ie}(r)$ is obtained via numerical solution of the HNC equations as a function of the direct electron-electron pair correlation function $g_{ee}(r)$, which is calculated separately. Aside from normalization, the impurity-electron pair correlation function is the average electron number density, $n_e(r)=n_e g_{ie}(r)$ at a distance r from the ion. Both MD simulation and the HNC approximation are restricted to a limited range of values of the impurity charge, density, and temperature. Outside this range, frequent electron trapping in MD, and nonconvergent iterative solutions in the case the HNC equations, could invalidate the results.

Nevertheless, within the parameter space considered here, MD and HNC results are in good agreement, as it is illustrated in Fig. 1. The enhanced electron accretion around the ion impurity is driven by classical attractive interaction mechanisms since the average number of electrons at a distance closer than δ is small, implying that the effect of the particular choice of regularization is negligible. Actually, the number of close electrons $n=g_{ie}(0)(\delta/r_0)^3$ is even smaller in the high-temperature case considered later on, where $n<10^{-2}$ for $Z=8$.

When the coupling to the ion is neglected the electron distribution becomes uniform regardless of the electron-electron coupling. Thus, the independent electron model is clearly a bad approximation for the electron density, except for $Z=0$. On the other hand, one can see in Fig. 1 the result found when the ion-electron interactions are included, but the electron-electron interactions are neglected. In this case, large-distance screening effects due to electron coupling are missed. In the particular case shown on Fig. 1, the electron coupling is small, approximately $\Gamma=0.116$, and the simple addition of Debye screening to the ion-electron interaction leads to quite good results.

Other properties involving the local electron electric field at the impurity are of primary interest for spectroscopy, since they determine the dipole coupling to the internal states of the emitter. The electric field can be determined from the gradient of the potential in Eq. (2). In the following, whenever the independent electron approximation is used, the screening of this field is changed to the Debye length.

Molecular dynamics results for the microfield distribution function $P(E)$ are illustrated for two values of impurity charge $Z=1$ and $Z=8$ in Fig. 2. It can be seen that the effect of increasing Z is to lower and broaden the distribution. The result for independent electrons, which corresponds to $Z=0$ is also shown in this figure and is close to the $Z=1$ MD result. As it was the case with the average electron density, the dominant Z dependence is due to the impurity-electron coupling. Nevertheless, for fixed Z the electron-electron coupling is responsible for quantitative changes of the distribution as the temperature is changed.

The simplest measure of the electric field dynamics is given by the field autocorrelation function. Figure 3 shows the time dependence for the cases $Z=1$ and $Z=8$ at $T_e=200\,000$ K and also shows the independent-electron limit. As it happened with the field distribution function, the last result is close to the $Z=1$ case. For low Z, the ad hoc screening of the fields assures that the covariance, $\langle E^2\rangle/E_0^2$, is similar to the value obtained taking into account electron-electron coupling. Debye screening also assures that the straight trajectory dynamics is effectively restricted to a De-

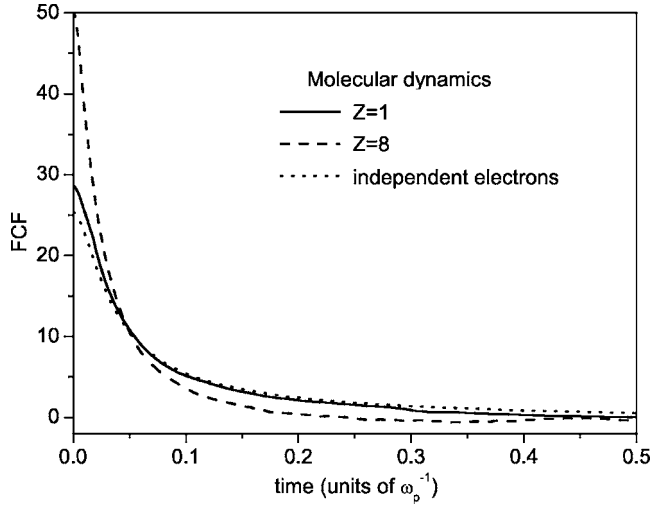

FIG. 3. Field autocorrelation function (same as Fig. 2).

bye sphere. However, the electron-impurity coupling changes this agreement dramatically at larger values of Z. Qualitatively, with growing Z the covariance increases, and correlation time decreases. Both these effects are missed by the independent electron approximation, but are regained qualitatively when impurity-electron coupling is introduced, even without electron-electron interactions. Even so, electron-electron coupling is required for quantitative effects indicated below.

The electron-impurity case of $Z=8$ is shown in more detail in Fig. 4. A striking feature, the anticorrelation (negative FCF) at intermediate times, appears. This effect gets more apparent for larger Z and lower temperature because of the enhanced electron-ion interactions. Many of these interactions lead to temporary orbiting trajectories with large oscillatory electric fields associated to them, which result in anticorrelation as it is observed in Fig. 4. In contrast to noninteracting electrons, constant energy exchanges assure a good phase-space sampling for coupled electrons. Thus, a correct equilibrium statistical sampling requires the electron-electron interactions to assure the properly weighted en-

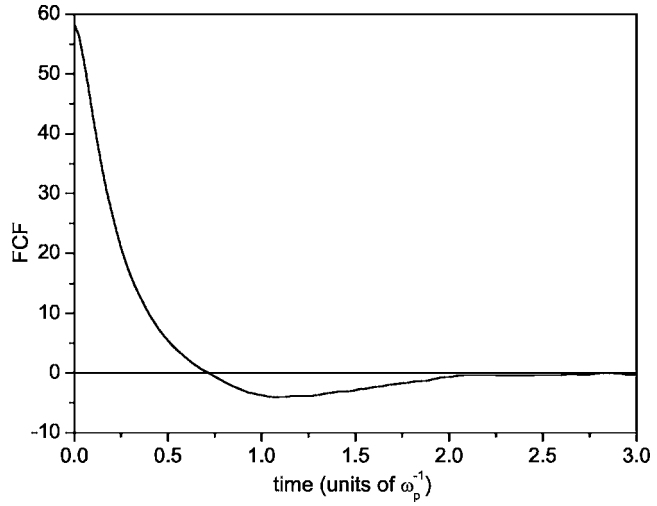

FIG. 4. FCF anticorrelation for $Z=8$ and $T_e=100\,000$ K.

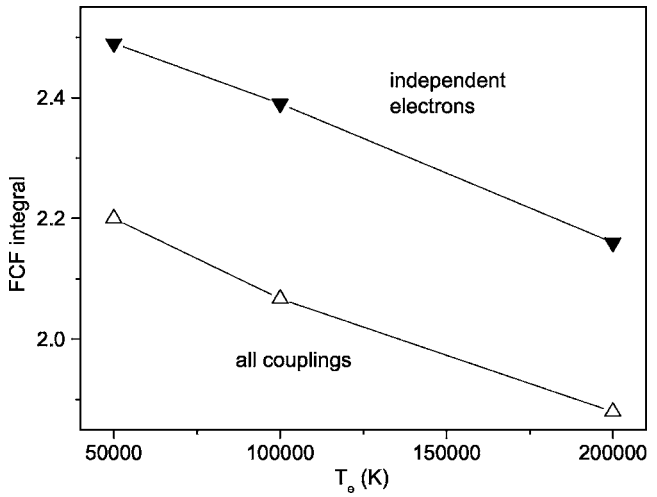

FIG. 5. FCF integral vs temperature for $Z=1$. White triangles: all couplings; black triangles: independent electrons.

semble of *temporary* orbiting trajectories.

It will be seen later that the spectral linewidth is proportional to the time integral of the FCF. It is difficult to predict, *a priori*, the Z dependence of this integral, due to the competing effects of increasing initial value and decreasing correlation time. Time integrals of the FCF are shown as a function of temperature in Fig. 5, which also includes the results corresponding to the independent particle model. It can be seen that the FCF integral decreases with temperature, so, evidently, the dynamical effect of a decreasing correlation time dominates, increasing initial field correlations. The effects of electron-impurity and electron-electron couplings lead to a $\sim 15\%$ decrease in the integral at all temperatures, relative to the result obtained in the independent electron model.

Finally, the Z dependence of the FCF integral is demonstrated in Fig. 6. Again dynamical effects of a decreasing correlation time and anticorrelation are dominant, leading to

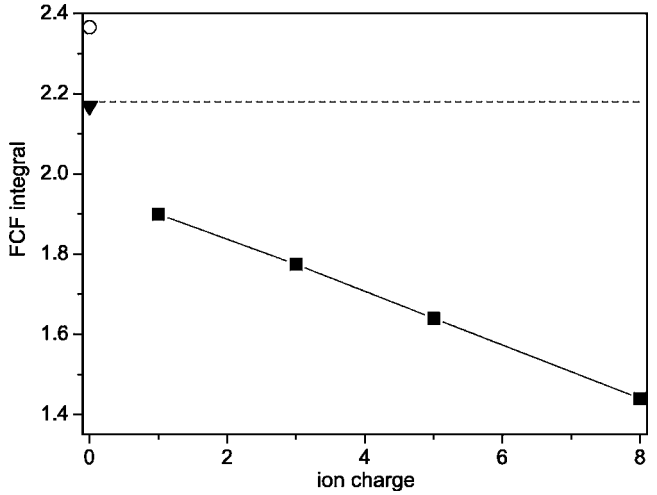

FIG. 6. FCF integral vs emitter charge at $T_e=200\,000$ K. Squares: all couplings; dashed: independent electrons; triangle: all couplings with $Z=0$; circle: unscreened uncoupled electrons with $Z=0$.

an approximately linear decrease of the integral with increasing Z. Considering first the value $Z=0$ (no impurity-electron interactions), the triangle represents the result where electron-electron coupling is included, whereas the dashed line corresponds to the independent electron model. It can be seen that the use of a Debye-screened field in the latter model accounts well for the relevant electron-electron coupling. This is consistent with the discussion following Fig. 3. On the other hand, the result corresponding to an independent-electron model without screening in shown with an open circle. It shows clearly that electron-electron coupling is almost a 10% effect at $Z=0$. This is significant since the electron-electron coupling constant is rather small ($\Gamma=0.029$). For $Z=1$ the electron-emitter interaction is quite important, decreasing the integral to a value almost 15% below the independent electron value. Electron-emitter coupling continues to dominate for increasing Z. As it was mentioned above, for $Z>0$ an additional factor that makes electron-electron coupling relevant in molecular dynamics is the need to establish the correct weight for the increasing number of quasibound orbits.

Some comments should be made on the conditions of the calculations leading to the results on Fig. 6. Typically, simulations involving neutral emitters are about two or three orders faster than those with a unique charged emitter. In order to carry out simulations with an equivalent residual noise for charged impurities and neutral emitters, the number of electrons involved in calculation is set smaller. This optimization—a decrease of the simulation cell size—intended to limit calculation cost, could cause a slight underestimate of the results with all couplings included (squares). Clearly, such a behavior could be fixed doing more expensive simulations.

III. ELECTRON-ION COUPLING EFFECTS ON LINE SHAPE

A. Dipole relaxation mechanisms

The dipole relaxation of a quantum emitter in a classical plasma environment can be deduced using linear-response methods under the hypothesis noted in the introduction and in the the case of no quenching conditions [1]. The spectral profile of dipole spontaneous emission is given in terms of the autocorrelation function $C(t)$ of the dipole moment $\mathbf{d}(t)$, via a Fourier transformation

$$I(\omega) = \mathrm{Re}\,\frac{1}{\pi}\int_0^\infty dt C(t) e^{\mathrm{i}\omega t}, \tag{3}$$

$$C(t) = tr\{U^+(t)\rho\mathbf{d}U(t)\cdot\mathbf{d}\}. \tag{4}$$

The trace in Eq. (4) is taken over an equilibrium Gibbs statistical ensemble ρ for the total system of plasma and emitter. The Hamiltonian is taken to be the sum of the plasma Hamiltonian (including the point monopole of the emitter) H_p, the Hamiltonian for the internal states of the emitter H_o, and a term describing the coupling of the plasma electric field with the internal emitter dipole. For simplicity, the Doppler broadening due to center of mass motion of the emitter has been assumed to be statistically independent of the dipole broadening due to the interaction with the plasma.

The operator $\mathbf{d}(t) \equiv U(t)\mathbf{d}U^+(t)$ obeys the Heisenberg equation

$$i\hbar\frac{d}{dt}\mathbf{d}(t) = (H_o - e\mathbf{E}(t)\cdot\mathbf{R}, \mathbf{d}(t)). \tag{5}$$

The second term in the commutator describes the perturbation due to the total electric field of the plasma $\mathbf{E}(t)$. In the no-quenching approximation, $e\mathbf{R}$ is restricted to the part of the internal emitter dipole operator coupled to the plasma field. The time dependence of $\mathbf{E}(t)$ is generated by the plasma Hamiltonian alone. This shows most directly the usefulness of MD simulations when addressing the most difficult part of a line-broadening problem: properly and completely identifying the environment of the emitter.

To represent an equilibrium ensemble for the environment, one must find a collection of field histories for different initial conditions, solve the Schrödinger equation (SE) in each case, and perform a simple algebraic average over all such solutions to get the line profile. In practice, the numerical solution of the Schrödinger equation can be either straightforward or complicated, depending on the electric field history. It is complicated for high Z radiators, since the quasibound orbits described above can give rise to high-frequency, strong fields. Then the calculation requires a fast integration process based on a polynomial development using the so-called Euler-Rodrigues coefficients. A detailed presentation of the method applied to hydrogenic lines has been given elsewhere [19].

A more compact formulation of the problem is achieved using a Liouville operator representation [20], which allows one to disentangle the evolution operator from the internal emitter dipole operator $\mathbf{d}$. Liouville operators are defined according to the following relation: $L_{0\cdot} \equiv (1/i\hbar)[H_0, \cdot]$. In this representation the dipole correlation function can be rewritten $C(t) = \mathrm{Tr}[\mathbf{d}\cdot U(t)\rho\mathbf{d}]$, and Eq. (5) is replaced by the following stochastic equation for the evolution operator alone

$$\frac{d}{dt}U_\alpha(t) = [L_0 + e\mathbf{E}_\alpha(t)\cdot\mathbf{R}]U_\alpha(t), \quad U_\alpha(0) = 1$$

$$\boldsymbol{\mathcal{U}}(t) = \{U_\alpha(t)\}_{av} = \frac{1}{N}\sum_{\alpha=1}^{N} U_\alpha(t), \tag{6}$$

where $\mathbf{E}_\alpha(t)$ is one of the electric field histories, $e\mathbf{R}$ is the Liouville representation of $e\mathbf{R}$ and $\boldsymbol{\mathcal{U}}(t)$ denotes the solution of the stochastic equation.

A useful approximation, described in the Appendix, is the fast fluctuation limit (FFL), and it can be used when the characteristic time for the field correlation function is much smaller than the typical relaxation time of the physical process investigated—here, the dipole relaxation due to the perturbation [21]. In the FFL, the stochastic equation reduces to

TABLE I. Balmer alpha FWHM (s^{-1}) versus temperature for $Z=1$.

Temperature (K)	γ_{FFL}	γ_{SE}
50000	10.7×10^{12}	11.8×10^{12}
100000	9.88×10^{12}	10.2×10^{12}
200000	9.32×10^{12}	9.93×10^{12}

$$\frac{d\mathcal{U}(t)}{dt} = (L_0 - \mathbf{W})\mathcal{U}(t), \tag{7}$$

where $\mathbf{W}$ is proportional to the field correlation function integral $\int_0^\infty \{\mathbf{E}_\alpha(0)\cdot\mathbf{E}_\alpha(t)\}_\alpha dt$. Then questions regarding the effects of charge-charge coupling on the linewidth can be addressed directly from the simulation of the field autocorrelation function as described in the previous section.

B. Electron broadening

The discussion of the magnitude of charge-charge coupling effects in electron broadening, i.e., in the full width at half maximum (FWHM), has been motivated, in part, by recent experimental and theoretical studies performed on a series of lines emitted by ions of increasing charge [9]. The specificity of these lines relies on the absence of ion broadening. In contrast, the present study concerns lines with ion broadening so the generalization of the results of this work to all lines could be questionable. Ion lines with significant ion broadening have been selected also as they fit the objective of studying Stark broadening in two-component plasmas, accounting for complete charge-charge coupling.

In the case under study, the simulation of dipole relaxation requires samples much longer than those necessary to obtain the field statistical properties. Moreover, since the dipole response of the emitter decreases as $1/(Z+1)^2$, high Z cases require integration of the Schrödinger equation over larger samples than for $Z=1$. The FFL allows a simpler theoretical representation of the linewidth, avoiding the full integration process. However, to check the results, the dipole autocorrelation has been calculated in a few cases by a complete integration of the Schrödinger equation.

In order to probe the statistical properties of the local microfield, Balmer-α lines for hydrogenlike emitters of charge $Z=1,3,5,8$ have been selected, together with the three plasma temperatures $T=50\,000$, $100\,000$, $20\,000$ K. The dipole moments of both the lower- and upper-level manifolds are coupled to the perturbing field, giving rise to the relaxation process and to the line broadening of the dipole transition $n=3\rightarrow n=2$. Qualitatively, for the Balmer-α line, the electric field perturbation induces two opposite broadening mechanisms, that is, an increase of broadening due to growing covariance of the field strength, and on the other hand, a decrease of broadening with increasing fluctuation dynamics of the perturbation, due to some time averaging inherent to the dipole relaxation mechanism.

The values of the FWHM for $Z=1$ are reported In Table I, where γ_{FFL} is the result of the fast fluctuation limit and γ_{SE} is the result of a full integration of the Schrödinger equation. The discrepancy between both methods is smaller than 10%. In addition, it is worth to mention that the exponential decay of $C(t)$, predicted by the FFL, is also confirmed in the simulations.

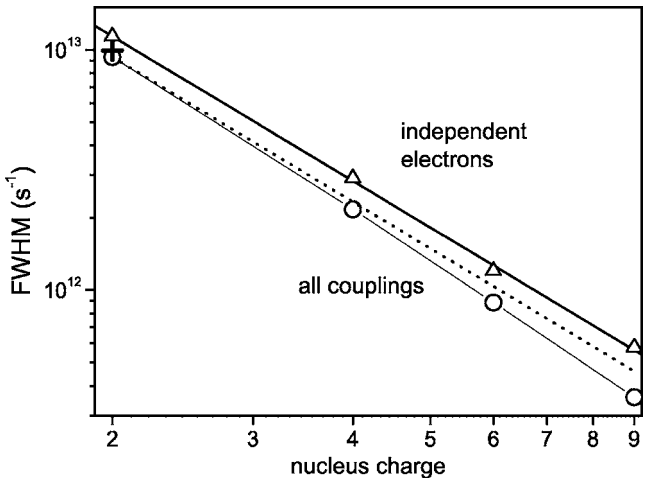

FIG. 7. Balmer-α FWHM, $Z=1$, 3, 5, and 8, $T_e=200\,000$ K. triangles: independent-electrons; solid line: independent-electron linear fit; circles: charge-charge coupling; cross: complete integration; dots: $1/(Z+1)^2$ line.

The results corresponding to the high temperature case are plotted on a log scale in Fig. 7 together with the outcome of independent electron calculations (electrons moving on straight trajectories and perturbing the emitter via a Debye-screened potential). The field sample generation cost in the MD technique is quite low for noninteracting particles. Therefore, these calculations can be performed by integration of the stochastic equation with a satisfactory noise level. The resulting FWHM calculations fit very well the $1/(Z+1)^2$ behavior (solid line) that represents the Z dependence of the linewidth through the dipole matrix elements. As in this case, the field autocorrelation function is independent of Z. These independent electron calculations validate the fast fluctuation limit approximation. The entire discrepancy between the two results of Fig. 7 is, therefore, a consequence of the charge-charge coupling in the time integral of the FCF as a function of the emitter charge (i.e., the effect considered in the discussion of Fig. 6). As it was shown in Fig. 5, this discrepancy will also increase with decreasing temperature.

Finally, it has been shown elsewhere that classical two-component MD simulations also provide relevant results regarding charge structure and dynamics [22]. In the case of two-component plasmas, the associated protocol designed to predict line spectra accounting for all couplings requires a numerical cost smaller than for the impurity case, given that several emitters are processed at the same time. In addition, because of increased broadening by the ions, the integration times are shorter. A comparison carried out assuming a Debye screening for the ion-ion potential and free electrons moving on straight trajectories shows a noticeable residual decrease of 6–7 % in the full width at half maximum when both the ion-electron and the electron-electron coupling are taken into account.

IV. CONCLUSION

Semiclassical models involving a quantum emitter perturbed by a stochastic classical electric field have been developed to calculate emitter dipole relaxation. Attention is focussed on relaxation by the electrons. On this basis, charge correlation effects at the lineshape level have been explored. Such reference results from ideal numerical experiments are indispensable, particularly when the plasma conditions are such that the usual theoretical approximations appear questionable. Calculations for two distinct models are reported here, with and without ion-electron and electron-electron couplings. The observed FWHM discrepancies confirm that the effect of charge-charge coupling, usually ignored for electron broadening beyond a screening effect, is not negligible. The test has been carried out on a line of interest for plasma spectroscopy—the Balmer α line—chosen because it matches the fast fluctuation limit conditions. The main result shows that the model without coupling overestimates the electron width by $\sim 10\%$. It should be emphasized that this conclusion stands only for the emission lines and plasmas considered in this study.

Classical molecular-dynamics simulations designed for ion and electron systems have been performed. For that purpose a regularized ion-electron potential has been used. Owing to the density temperature conditions this pure classical approach appears relevant: the short-distance regularization procedure based on the De Broglie wavelength is expected not to significantly affect the coupling effect observed on the line shapes. For the plasma itself it has been shown that the electron-electron interactions play a major part if the ion-electron interactions are accounted for. Both contribute to obtain the correct statistical behavior of the electric forces at the ion. In terms of the electric field dynamics, these couplings induce an increase of both the covariance and the field fluctuation rate when the emitter charge or the temperature increases.

ACKNOWLEDGMENTS

Support for this research has been provided, in part, by French and Spanish collaboration plan (PAI Picasso). The Spanish group has been financed by de DGICYT (projects No. FTN2001-1827 and No. ENE2004-05038/FTN) and the Junta de Castilla y León (Project No.VA009/03). The research of J. Dufty was supported by U. S. Department of Energy Grant No. DE-FG02ER54677 and by the University of Provence.

APPENDIX: FAST FLUCTUATION LIMIT

The terminology "fast fluctuation limit," used instead of the alternative "impact limit," has been preferred to avoid confusion with impact theories, which rely on the calculation of an average binary collision—the collision operator. Impact theories generally postulate nonoverlapping strong collisions, which is not a limitation of the fast fluctuation limit obtained here.

1. Characteristic time scales

Three characteristic time scales have to be considered. First, the typical correlation time of the perturbing field $\mathbf{E}(t)$ and, in consequence, the characteristic time of $L(t)$. This time scale is ruled by the kinetics of the charged particles in the plasma. Its order of magnitude is

$$\tau_c \simeq \frac{r_0}{v_0}, \tag{A1}$$

where r_0 denotes typical inter-particle distance and v_0 mean thermal velocity.

A second time scale is fixed by the correlations of the dipole-moment $\mathbf{d}(t)$. The spectral width is determined by this lifetime τ_d, which is, in a way, the "unknown variable" of the problem.

Finally, a last time scale is fixed by characteristic values of L

$$\frac{1}{\tau_H} \simeq L \simeq \frac{1}{\hbar} e E_0 \frac{n^2 a_0}{Z}, \tag{A2}$$

where a_0 is the Böhr radius and n the principal quantum number of the upper group of states. Evolution of the dipole moment $\mathbf{d}(t)$ would be fixed by this frequency scale if the perturbing electric field were stationary.

The relationship between τ_H and τ_c will determine the relevant physical phenomenon in spectral line broadening. $\tau_c \geqslant \tau_H$ is the condition for "quasistatic" broadening, which is a close limit for ion broadening. In this case both shape and width of the spectral line are fixed by the statistical distribution of the perturbing fields, then $\tau_d \sim \tau_H$.

If $\tau_c \ll \tau_H$ the evolution of the dipole moment $\mathbf{d}(t)$ is much slower than the evolution of the perturbing fields. Electron-broadening mechanisms satisfy this condition. Then, perturbations are less efficient, since the emitter responds to a time average of the electric field smaller than its statistical typical value. It is the fast fluctuation regime. In the next section it will be seen that in this regime the dipole autocorrelation fits well a decreasing exponential whose lifetime $\tau_d \gg \tau_H > \tau_c$, is determined by the autocorrelation function of the perturbing field. It should be noted that in the present study the ratio τ_c / τ_d varies from a few hundred to a few thousand. Such a large ratio guarantees that the FFL is totally relevant because the discrepancy between the dipole autocorrelation function and an exponential (or equivalently the discrepancy between the line shape and Lorentzian) is nonsignificant.

2. Fast fluctuation limit

The dipole correlation function can be rewritten as

$$C(t) = tr\{\mathbf{d}(t) \cdot \mathbf{d}\rho\} = tr_0(tr_p\{e^{Lt}\rho\mathbf{d}\} \cdot \mathbf{d}), \tag{A3}$$

after separating the trace into that for the emitter and plasma subspaces, using stationarity of the Gibbs ensemble under the dynamics and introducing the Liouville operator $L = L_0 + L_p + L_i$ generating the dynamics. L is the sum of the Liouville operator for the emitter in the relative coordinate system L_0, the Liouville operator for the plasma including the center of mass (point monopole) of the emitter L_p, and the coupling

between the internal emitter states and the plasma L_i.

The interaction representation generator is defined by

$$e^{Lt} = e^{(L_0+L_p)t}U(t) = e^{(L_0+L_p)t}T\exp\int_0^t dt' L_i(t'). \quad \text{(A4)}$$

Here T is the time-ordering operator with largest times to the left. Then,

$$C(t) \equiv tr_0(e^{(L_0+L_p)t}e^{\hat{O}(t)}f_0\mathbf{d})\cdot\mathbf{d}, \quad \text{(A5)}$$

where $\hat{O}(t)$ is the average generator for the interaction dynamics in the atomic subspace

$$e^{\hat{O}(t)} = tr_p T\exp\int_0^t dt' L_i(t')\rho f_0^{-1} = \left\langle T\exp\int_0^t dt' L_i(t')\right\rangle_p, \quad \text{(A6)}$$

where $f_0 = tr_p\rho$

The leading terms in a cumulant expansion of this average are

$$\hat{O}(t) = \hat{O}^{(1)}(t) + \hat{O}^{(2)}(t) + \cdots \quad \text{(A7)}$$

with

$$\hat{O}^{(1)}(t) = \int_0^t dt' \langle L_i(t')\rangle_p \quad \text{(A8)}$$

$$\hat{O}^{(2)}(t) = \int_0^t dt\int_0^{t'} dt''\langle\tilde{L}_i(t')\tilde{L}_i(t'')\rangle_p = t\int_0^t dt'\left(1-\frac{t'}{t}\right)\langle\tilde{L}_i(t)\tilde{L}_i(t')\rangle_p, \quad \text{(A9)}$$

where $\tilde{L}_i(t') = L_i(t') - tr_p L_i(t')\rho f_0^{-1}$.

The fast fluctuation limit corresponds to the case where the perturber dynamics varies rapidly on the time scale of the dipole correlation function $C(t)$. Since the average is performed only over the plasma degrees of freedom this time scale is controlled by the perturbers. Then the fluctuation in Eq. (A9) decays to zero for $t' = \tau \ll t$ and the factor t'/t in the integrand can be neglected

$$\hat{O}^{(2)}(t) \to t\int_0^t dt'\langle\tilde{L}_i(t)\tilde{L}_i(t')\rangle_p. \quad \text{(A10)}$$

For similar reasons, higher-order terms in the cumulant expansion are expected to be of higher order in τ/t and, therefore, negligible.

Further simplifications occur with additional assumptions. If the interaction is only through a coupling of the emitter dipole to the plasma field then $L_i = -e\mathbf{E}\cdot\mathbf{R}$. Also, if the emitter-plasma interactions are neglected in ρf_0^{-1} then $\rho f_0^{-1} \to \rho_p$ and the fluctuations become

$$\langle L_i(t)\rangle_p \to 0,$$

$$\langle\tilde{L}_i(t)\tilde{L}_i(t')\rangle_p \to \frac{e^2}{3}G_E(t-t')\mathbf{R}(t)\cdot\mathbf{R}(t'), \quad \text{(A11)}$$

where $G_E(t)$ is the electric field autocorrelation function for the plasma alone

$$G_E(t) = \langle\mathbf{E}(t)\cdot\mathbf{E}(\mathbf{0})\rangle_p \quad \text{(A12)}$$

and the dipole operator in $\mathbf{R}(t)$ has a time dependence due to the emitter alone. Finally, in the case of an emitter with upper and lower degenerate manifolds, such as the Balmer-α line without fine structure this time dependence of the dipole operators can be neglected as well. The result quoted in the text is then obtained

$$C(t) \equiv tr_0(e^{L_0 t}e^{t[\int_0^\infty dt'(e^2/3)G_E(t')\mathbf{R}\cdot\mathbf{R}]}f_0\mathbf{d})\cdot\mathbf{d}. \quad \text{(A13)}$$

[1] H. R. Griem, *Spectral Line Broadening by Plasmas* (Academic Press, New York, 1974).

[2] D. Voslamber, Z. Naturforsch. A **24**, 1458 (1969); E. W. Smith, J. Cooper, and C. R. Vidal, Phys. Rev. **185**, 140 (1969).

[3] H. R. Griem, A. C. Kolb, and K. Y. Shen, Phys. Rev. **116**, 4 (1959); H. R. Griem, A. C. Kolb, and K. Y. Shen, Astrophys. J. **135**, 272 (1962).

[4] S. Alexiou, Phys. Rev. A **49**, 106 (1994); S. Alexiou and Y. Maron, J. Quant. Spectrosc. Radiat. Transf. **53**, 109 (1995).

[5] R. Stamm, B. Talin, E. L. Pollock, and C. A. Iglesias, Phys. Rev. A **34**, 4144 (1986).

[6] M. A. Gigosos, M. A. González, and V. Cardeñoso, Spectrochim. Acta, Part B **58**, 1489 (2003).

[7] For practical reasons the word "coupling" is equally used to mention plasma conditions (e.g., *weak plasma coupling*) and the interactions strengths themselves (e.g., *electron-electron coupling*).

[8] H. R. Griem, Contrib. Plasma Phys. **40**, 46 (2000).

[9] Yu. V. Ralchenko, H. R. Griem, and I. Bray, J. Quant. Spectrosc. Radiat. Transf. **81**, 371 (2003); H. Hegazy, S. Seidel, Th. Wrubel, and H.-J. Kunze, *ibid.* **81**, 221 (2003).

[10] H. Minoo, M.-M. Gombert, and C. Deutsch, Phys. Rev. A **23**, 924 (1981).

[11] J. P. Hansen and I. R. McDonald, Phys. Rev. A **23**, 2041 (1981); G. E. Norman, A. A. Valuev, and I. A. Valuev, J. Phys. IV **10**, Pr5–255 (2000); T. Pschiwul and G. Zwicknagel, Contrib. Plasma Phys. **41**, 271 (2001).

[12] J. P. Hansen, I. R. McDonald, and E. L. Pollock, Phys. Rev. A **11**, 1025 (1975).

[13] F. J. Rogers, J. Chem. Phys. **73**, 6272 (1980); Phys. Rev. A **29**, 868 (1984).

[14] B. Talin, A. Calisti, and J. Dufty, Phys. Rev. E **65**, 056406 (2002).

[15] L. Collins, I. Kwon, J. Kress, N. Troullier, and D. Lynch, Phys. Rev. E **52**, 6202 (1995).

[16] M. W. C. Dharma-wardana, in *Strongly Coupled Plasmas*, edited by H. de Witt and F. Rogers (NATO ASI Series, Plenum, NY, 1987), Vol. 275.

[17] F. Perrot and M. W. C. Dharma-wardana, Phys. Rev. A **30**, 2619 (1984).

[18] J. W. Dufty, I. Pogorelov, A. Calisti, and B. Talin, J. Phys. A **36**, 6067 (2003); J. W. Dufty, I. Pogorelov, A. Calisti, and B. Talin, Phys. Rev. E (to be published).

[19] M. A. Gigosos, J. Fraile, and F. Torres, Phys. Rev. A **31**, R3509 (1985); M. A. Gigosos and V. Cardeñoso, J. Phys. B **20**, 6005 (1987); M. Gigosos and V. Cardeñoso, J. Phys. B **29**, 4795 (1996).

[20] U. Fano, Phys. Rev. **131**, 259 (1963).

[21] M. Lewis, Phys. Rev. **121**, 501 (1964); C. Cohen-Tannoudji, *Aux Frontières de la Spectroscopie Laser*, Vol. 1, (North-Holland, Amsterdam, 1975).

[22] B. Talin, E. Dufour, A. Calisti, M. A. Gigosos, M. A. González, T. del Río Gaztelurrutia, and J. W. Dufty, J. Phys. A **36**, 6049 (2003); E. Dufour, A. Calisti, B. Talin, M. A. Gigosos, M. A. González, and J. W. Dufty, J. Quant. Spectrosc. Radiat. Transf. **81**, 125 (2003).